On an analytical orthonormal multipolar basis for magnetic anomaly detection

Clément Chenevas-Paule, Steeve Zozor, L-L. Rouve, Olivier J.J. Michel, Olivier Pinaud, Romain Kukla

On an analytical orthonormal multipolar basis for magnetic anomaly detection

C. Chenevas-Paule*†‡§, S. Zozor*§, L.-L. Rouve†§, O.J.J. Michel*§, O. Pinaud†§ and R. Kukla‡§
* Univ. Grenoble Alpes, CNRS, Grenoble INP, GIPSA-Lab, 38000 Grenoble, France
† Univ. Grenoble Alpes, CNRS, Grenoble INP, G2Elab, 38000 Grenoble, France
‡ Centre d'Expertise pour la Maîtrise de l'Information et des Signatures, Naval Group, Ollioules, France
§ Naval Electromagnetism Laboratory, 21 avenue des Martyrs, 38000 Grenoble, France

***Abstract*—Magnetic anomaly detection aims to find hidden ferromagnetic masses by estimating the weak perturbation they induce on local Earth's magnetic field. Classical detection schemes rely on signals recorded on a moving sensor, and the modeling of the source as a function of unknown parameters. These are eased if the source field along the magnetometer trajectory decomposes over an orthonormal basis. Usually, spherical harmonics are used for determining the general multipolar basis functions that describe the anomaly signal. A new analytical set of functions (multipolar orthonormal basis functions - MOBF) that spans the space of the noise-free measured signal is introduced in this paper. The sampled MOBF are shown to satisfy quasi orthonormality, providing fairly equivalent performances than those obtained after a Gram-Schmidt orthonormalization on the sampled initial basis.**

***Index Terms*—Magnetic Anomaly Detection, Harmonic Multipolar Decomposition, Multipolar Orthonormal Basis Functions**

I. Introduction

Magnetic anomaly detection (MAD) consists in analyzing a measured local magnetic field to assess the presence of hidden weak magnetic sources and is used for various applications (detection of under water pipes or cables, wrecks, submarines, etc). MAD is based on the analysis of a recorded signal from a magnetometer on board an aircraft flying over the ocean surface. Algorithms based on orthogonal basis functions (OBF) are widely studied [1]–[4] to derive efficient detection methods, that mostly lead to develop a generalized likelihood ratio test (GLRT) on the projected signal onto the OBF. In the far field assumption, the magnetic source is accurately modeled by a magnetic dipole. In a more realistic framework where this assumption is no longer satisfied, the problem has been revisited in [5] [6, Sec. 3.12] and a spherical harmonic (SH) expansion of the magnetic induction $\boldsymbol{B}$ has been used as follows:

$$\boldsymbol{B}(P) = -\mathbf{grad}\left(\frac{\mu_0}{4\pi}\sum_{l=1}^{+\infty}\frac{1}{r^{l+1}}\sum_{m=0}^{l}\big(a_{l,m}\cos(m\phi) + b_{l,m}\sin(m\phi)\big)\mathcal{P}_l^m(\cos\theta)\right) \quad (1)$$

where (r,θ,ϕ) are the spherical coordinates of P assuming that the source is placed at the origin of the reference system, $\mathcal{P}_l^m$ denote the associated Legendre polynomials. The truncation of Eq. (1) has allowed to propose a general multipolar basis, orthonormlized with a Gram-Schmidt process, that efficiently represents the signal. In the sequel, we will call this basis "multipolar orthonormal basis functions" (MOBF). Our contribution is twofold. First, a direct approach (avoiding SH expansion) is proposed to recover the basis of [5], spanning the space of the multipolar signal along the sensor trajectory. Secondly, an analytical derivation of the MOBF is presented, based on orthogonal polynomial theory. The advantage of this derivation is the avoidance of numerical Gram-Schmidt (GS) orthogonalization, known to be potentially numerically unstable in large dimensions, or of more complex orthonormalization procedures [7]. As this approach is theoretically desired for expressing true signals, sampling effect is studied, as well as the effect of GS on the sampled MOBF. Finally, the behavior of the three sets of functions (sampled MOBF, numerical orthonormalization of the sampled initial basis or MOBF) in the detection performance will be briefly illustrated through a simulated example.

II. Magnetic Anomaly Detection problematic

A. The detection problem – A reminder

The detection problem is classically formulated as a binary hypothesis testing problem:

$$\begin{cases}\mathcal{H}_0: & \boldsymbol{x} = & \boldsymbol{n} & \text{(absence of the target)}\\ \mathcal{H}_1: & \boldsymbol{x} = & \boldsymbol{s}+\boldsymbol{n} & \text{(presence of the target)}\end{cases} \quad (2)$$

where noise $\boldsymbol{n}$, measurement $\boldsymbol{x}$ and signal $\boldsymbol{s}$ to be detected are matrices of $\mathbb{R}^{d\times K}$, K being the number of samples and d the measurement dimension (i.e. $d=3$ for triaxial magnetometer). All the non-source signals are embedded in the noise, modeling geomagnetism phenomena, instrumental uncertainties or motion related instabilities. Such a problem is widely documented and the Bayes optimal solution (w.r.t. a cost function related

to some decision error) leads to compare the likelihood ratio (LR) or any monotonic transform of LR to a threshold [8]. For the model (2) at hand the probability density function (pdf) of $\boldsymbol{x}$ under $\mathcal{H}_1$ may involve an unknown parameter vector $\boldsymbol{\theta} \in \boldsymbol{\Theta}$ leading to the formulation of the generalized log-likelihood ratio test (GLLRT) [8], the latter taking the following expression when $\boldsymbol{\theta}$ is only involved in $\boldsymbol{s}$:

$$\max_{\boldsymbol{\theta}\in\boldsymbol{\Theta}} \Lambda(\boldsymbol{x} \,|\, \boldsymbol{\theta}) \equiv \log \left(\frac{p_{\boldsymbol{n}} \left(\boldsymbol{x} - \boldsymbol{s} \left(\widehat{\boldsymbol{\theta}}_{\text{mle}} \right) \right)}{p_{\boldsymbol{n}}(\boldsymbol{x})} \right) > \eta, \quad (3)$$

$p_{\boldsymbol{n}}$ being the noise pdf and where $\widehat{\boldsymbol{\theta}}_{\text{mle}}$ is the maximum likelihood estimator (MLE) of $\boldsymbol{\theta}$,

$$\widehat{\boldsymbol{\theta}}_{\text{mle}} = \underset{\boldsymbol{\theta}\in\boldsymbol{\Theta}}{\operatorname{argmax}} \; p_{\boldsymbol{n}} \left(\boldsymbol{x} - \boldsymbol{s}(\boldsymbol{\theta}) \right) \quad (4)$$

The major drawback of such an approach is the requirement of the knowledge of both the noise pdf and the parametric (w.r.t. $\boldsymbol{\theta}$) model of the signal under $\mathcal{H}_1$. This motivates numerous studies where the departure from $\mathcal{H}_0$ only is considered. The purpose of this paper is different and put the emphasis on the target modeling. The noise contribution is assumed to be Gaussian, with independent and identically distributed components with variance σ^2, thus $p_{\boldsymbol{n}}(\boldsymbol{x}) = (2\pi\sigma^2)^{-\frac{Kd}{2}} \exp\left(-\frac{1}{2\sigma^2} \operatorname{Tr}\left(\boldsymbol{x}^t \boldsymbol{x}\right)\right)$. Consequently, the GLLRT reads:

$$\operatorname{Tr}\left(2\, \boldsymbol{s}\left(\widehat{\boldsymbol{\theta}}_{\text{mle}}\right) \boldsymbol{x}^t - \boldsymbol{s}\left(\widehat{\boldsymbol{\theta}}_{\text{mle}}\right) \boldsymbol{s}\left(\widehat{\boldsymbol{\theta}}_{\text{mle}}\right)^t \right) > \eta \quad (5)$$

with Tr and $\cdot^t$ the trace and transposition operators.

B. Source modeling – Multipole expansion

Our detection problem requires the modeling of the source signal. Remind that the sensor follows a rectilinear trajectory, at a constant altitude and constant speed, see Fig. 1. The coordinate system is centered at the source O, assumed to be motionless with respect to the sensor, so that the x-axis is parallel to sensor's trajectory and $x-y$ is the horizontal plane. The closest point to the source origin is called CPA (Closest Point of Approach). Let t_0 be the instant when the sensor is at the CPA, D the minimal source-sensor distance and β the angle made by the line (O-CPA) with the vertical axis.

Departing from the SH expansion in [5], we propose to use the field expression proposed by [9] valid outside the Brillouin sphere (BS):

$$\boldsymbol{B}(P) = \sum_{l\in\mathbb{N}^*} \boldsymbol{B}^{(l)}(P) \quad (6)$$

with

$$\boldsymbol{B}^{(l)}(P) = \frac{\mu_0}{4\pi} \frac{(2l+1)\left(\boldsymbol{r}\cdot\boldsymbol{M}^{(l)}\right)\boldsymbol{r} - l\, r^2 \boldsymbol{M}^{(l)}}{r^{l+4}} \quad (7)$$

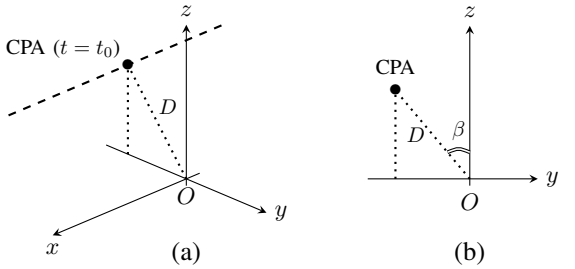

Fig. 1. Geometry of the problem. Center of the target is located at O, sensor P moves along the dashed line. D is the distance between the CPA and the source location, and is reached at time t_0 by the sensor. (a) perspective view and (b) view in the $y-z$-plane.

where $\boldsymbol{M}^{(l)}$ is a vector resulting from the Einstein product [10], [11] between an l-order[1] symmetric traceless tensor $\boldsymbol{m}^{(l)}$ of size 3 in each dimension and the unitary $\boldsymbol{u}_r = \frac{\boldsymbol{r}}{r}$ to the $(l-1)$-th tensor power,

$$\boldsymbol{M}^{(l)}(P) = \frac{\boldsymbol{m}^{(l)} *_{l-1} \boldsymbol{r}^{\otimes(l-1)}}{l!\, r^{l-1}} \quad (8)$$

In the source cartesian coordinate system from Fig. 1, we get $\boldsymbol{r} = \begin{bmatrix} x & D\sin\beta & D\cos\beta \end{bmatrix}^t$, thus $r = \sqrt{x^2 + D^2}$. As the components of the tensor $\boldsymbol{r}^{\otimes(l-1)}$ are monomials in x of degree less or equal to $l-1$ (with a factor function of β), the numerator of $\boldsymbol{M}^{(l)}$ in Eq. (8) is a polynomial in x with degree lower or equal to $l-1$, with 3-dimensional constant coefficients depending on β and components of $\boldsymbol{m}^{(l)}$. Inserting Eq. (8) into (7), we finally obtain along the trajectory:

$$\boldsymbol{B}^{(l)}(u) = \frac{\displaystyle\sum_{n=0}^{l+1} \boldsymbol{\alpha}_n^{(l)} u^n}{\left(1+u^2\right)^{l+\frac{3}{2}}}, \quad u = \frac{x}{D} = \frac{V\,(t-t_0)}{D} \quad (9)$$

where the d-dimensional coefficients $\boldsymbol{\alpha}_n^{(l)}$ depend only on the tensor $\boldsymbol{m}^{(l)}$ and the angle β.

From now on, the magnetic field will be assumed to be produced by a finite number of multipoles N, or approximated by a truncation of order N. We additionally assume that the sensor does not rotate along the trajectory so that the projection of the coefficients $\boldsymbol{\alpha}_n^{(l)}$ on the sensor axes is constant w.r.t. u. Consequently, from the truncated Eq. (6) and Eq. (9), the sensor measurement along its trajectory reads:

$$\boldsymbol{s}(u) = \sum_{n=0}^{2N} \boldsymbol{a}_N^{(n)} f_{N,n}(u), \quad u = \frac{V\,(t-t_0)}{D} \quad (10)$$

where the set $\mathcal{F}_N = \left\{ f_{N,n} \right\}_{n=0}^{2N}$ of the $2N+1$ functions

$$f_{N,n} : \; u \mapsto \frac{u^n}{\left(1+u^2\right)^{N+\frac{3}{2}}} \quad (11)$$

forms a basis for the source space.

[1] ($l = 1$ corresponds to the dipole, $l = 2$ to the quadripole,...)

Note that:

- Coefficients $\boldsymbol{a}_N^{(n)}$ depend on the source and the trajectory (coordinate system orientation, angle β), and the basis functions $f_{N,n}$ on the trajectory through V, D, t_0.
- We recover the expression exhibited in [5] by using another formula for the multipolar field [9], [12], solution of the Laplace equation.
- The OBF inferred from a dipole source field [2], [3] are a particular case of the MOBF with $N = 1$.

In the sequel, parameters N, D and t_0 are assumed to be known. Their estimation is left as a perspective (see [2], [5] for this problem).

III. Source parameters estimation and induced detector

In practice, the measurements are sampled along the trajectory, so that Eq. (10) writes for the acquisition

$$\boldsymbol{s} = \boldsymbol{A}_N \boldsymbol{F}_N \tag{12}$$

where $\boldsymbol{A}_N = \begin{bmatrix} \boldsymbol{a}_N^{(0)} & \cdots & \boldsymbol{a}_N^{(2N)} \end{bmatrix} \in \mathbb{R}^{d\times(2N+1)}$ depends on the source and β, and $\boldsymbol{F}_N \in \mathbb{R}^{(2N+1)\times K}$ is the matrix whose rows are the sampled basis functions $f_{N,n}$, depending only on the trajectory.

From Eqs. (12), (4) and (5) we get $\widehat{\boldsymbol{\theta}}_{\text{mle}} \equiv \widehat{\boldsymbol{A}_{N\,\text{mle}}} = \operatorname{argmax}_{\boldsymbol{A}_N} \operatorname{Tr}\left(2\boldsymbol{A}_N\boldsymbol{F}_N\boldsymbol{x}^t - \boldsymbol{A}_N\boldsymbol{F}_N\boldsymbol{F}_N^t\boldsymbol{A}_N^t\right)$. Consequently, the MLE is solution of $\boldsymbol{A}_N\boldsymbol{F}_N\boldsymbol{F}_N^t = \boldsymbol{x}\boldsymbol{F}_N^t$. In practice, the number of samples $K \gg 2N+1$, and $\boldsymbol{F}_N$ is of full rank, as $\mathcal{F}_N$ is a basis of the source space. Therefore, the Gram-matrix $\boldsymbol{F}_N\boldsymbol{F}_N^t$ is nonsingular, so

$$\widehat{\boldsymbol{A}_{N\,\text{mle}}} = \boldsymbol{x}\,\boldsymbol{F}_N^t\left(\boldsymbol{F}_N\boldsymbol{F}_N^t\right)^{-1} \tag{13}$$

and the GLLRT Eq. (5) turns to be,

$$\operatorname{Tr}\left(\widehat{\boldsymbol{A}_{N\,\text{mle}}}\boldsymbol{F}_N\boldsymbol{F}_N^t\,\widehat{\boldsymbol{A}_{N\,\text{mle}}}^t\right) > \eta \tag{14}$$

the well-known energy detector. However, performing the detection requires a matrix inversion and studying the performance of the detector, at first glance, is not an easy task. It would be clearly easier if $\boldsymbol{F}_N$ were composed by orthonormal rows i.e., if $\boldsymbol{F}_N$ were a Stiefel matrix.

Previous studies realized an orthonormalization process thanks to the GS orthonormalization, as well as for the dipole case [2], [3] as for multipole one [5]. Let us write $\boldsymbol{F}_N^{\text{o}}$ a given matrix composed by orthonormal rows, and $\boldsymbol{A}_N^{\text{o}}$ the coefficient on this basis, so that Eqs. (13)–(14) reduce to the projection of the observation on $\boldsymbol{F}_N^{\text{o}}$, and to the energy receiver

$$\widehat{\boldsymbol{A}_{N\,\text{mle}}^{\text{o}}} = \boldsymbol{x}\boldsymbol{F}_N^{\text{o}\,t}, \qquad \left\|\widehat{\boldsymbol{A}_{N\,\text{mle}}^{\text{o}}}\right\|_F^2 > \eta \tag{15}$$

where $\|\boldsymbol{A}\|_F^2 = \operatorname{Tr}\left(\boldsymbol{A}\boldsymbol{A}^t\right)$ is the squared Froebenius norm. As the components of $\boldsymbol{n}$ are independent, Gaussian with variance σ^2, it turns out that $\|\boldsymbol{A}\|_F^2/\sigma^2$ follows a chi-squared law with $d(2N+1)$ degrees of freedom, with central parameter $\lambda_i = i\left\|\boldsymbol{s}\boldsymbol{F}_N^{\text{o}\,t}\right\|_F^2/\sigma^2$ under $\mathcal{H}_i$. This allows to write the theoretical probability of detection $P_{\text{d}} = \Pr[\Lambda > \eta|\mathcal{H}_1]$ and that of false alarm $P_{\text{fa}} = \Pr[\Lambda > \eta|\mathcal{H}_0]$ thanks to the cumulative density function of noncentral and central chi-squared variables, respectively [5].

Note that these results require an orthonormalization procedure instead of the matrix inversion involved in the receptor when no orthonormalization is performed. Moreover, in both cases, numerical errors can appear, especially when N becomes large. Furthermore, in the case where we have to perform the detection for various N (e.g., when unknown), the procedure is to be performed several times. Such a procedure could be avoided if an analytical orthonormal basis is found to express the signal. We show in the next section that such an expression exists, involving non classical orthogonal polynomials, although they can be indirectly linked to known ones.

IV. Construction of analytical multipolar orthonormal basis functions

A. Orthogonalization step

From Eq. (11), finding an orthonormal basis for the space spanned by $\mathcal{F}_N$ associated with the natural inner product in $\mathcal{L}^2(\mathbb{R})$ is totally equivalent to finding an orthonormal basis for the space of polynomials $\mathbb{R}_{2N}[X]$ of degree $2N$ associated with the following inner product:

$$\langle P|Q\rangle_{w_N} = \int_{\mathbb{R}} P(u)\,Q(u)\,w_N(u)\,du \tag{16}$$

where the weight w_N of this inner product is given by:

$$w_N(u) = (1+u^2)^{-2N-3} \tag{17}$$

w_N satisfies the required conditions for applying the Rodrigues formula [13, Eq. 22.1.6] to build a sequence $P_{N,n}$ of polynomials of degree n forming an orthonormal basis of $\mathbb{R}_{2N}[X]$ for the inner product (16)-(17), which writes here:

$$P_{N,n}(u) = c_{N,n}\,(1+u^2)^{2N+3}\,\frac{d^n}{du^n}(1+u^2)^{n-2N-3}$$

where $c_{N,n}$ is a normalization coefficient to be found.

Let us introduce $h : u \mapsto u^{n-2N-3}$ and $g : u \mapsto 1+u^2$. The n^{th} derivative term in the Rodrigues formula is $(h\circ g)^{(n)}$, i.e., that of a composite function which can be computed with the Faà di Bruno formula [14],

$$(h\circ g)^{(n)} = \sum_{\pi\in\Pi_n} h^{(|\pi|)}\circ g \prod_{B\in\pi} g^{(|B|)}$$

where Π_n denotes the set of partitions of $\{0,\ldots,n\}$ and $|\cdot|$ the cardinal of a set. Because $g^{(k)} = 0$ when $k > 2$, the non-zero terms are those given by the partitions whose elements have cardinal less or equal to 2. Iterating

over the number of doublets contained in each of such partitions allows us to finally obtain

$$P_{N,n}(u) = c_{N,n} \sum_{k=0}^{\left\lfloor \frac{n}{2} \right\rfloor} d_{N,n,k} (1+u^2)^k \, (2u)^{n-2k} \quad (18)$$

where $\lfloor \cdot \rfloor$ is the floor function and

$$d_{N,n,k} = \frac{(-1)^{n-k} \, n! \, (2N+2-k)!}{(n-2k)! \, k! \, (2N+2-n)!} \quad (19)$$

B. Normalization

Normalizing the basis means searching for $c_{N,n}$ such that

$$\int_{\mathbb{R}} P_{N,n}(u)^2 \, w_N(u) \, du = 1$$

The key idea here is to introduce the Rodrigues formula into only one factor $P_{N,n}$ in the integral and to repeat n successive integrations by part. The nullity of the all-inclusive terms leads to:

$$(-1)^n \, n! \, c_{N,n} \, p_{N,n} \int_{\mathbb{R}} (1+u^2)^{n-2N-3} \, du = 1 \quad (20)$$

where $p_{N,n}$ is the dominant coefficient of $P_{N,n}$. It just so happens that it is easy to find it by using binomial formula into (18)-(19):

$$p_{N,n} = c_{N,n} \, n! \sum_{k=0}^{\left\lfloor \frac{n}{2} \right\rfloor} \frac{(-1)^{n+k} \, 2^{n-2k} \, (2N+2-k)!}{(n-2k)! \, k! \, (2N+2-n)!}$$

It appears that the sum is a Gegenbauer polynomial evaluated at point 1 whose value is known [13, Eqs. 22.3.1, 22.4.2], leading to,

$$\begin{aligned} p_{N,n} &= c_{N,n} \, n! \, (-1)^n \, C_n^{(2N+3-n)}(1) \\ &= c_{N,n} \, n! \, (-1)^n \binom{4N+5-n}{n} \end{aligned}$$

Inserting this result into (20) and calculating the integral term [13, § 6.2] we get:

$$c_{N,n}^2 = \frac{4^{2N-n+2} \, (4N+5-2N)! \, (2N-n+2)!}{\pi \, n! \, (4N+5-n)! \, (4N+4-2n)!} \quad (21)$$

As a conclusion, $\mathcal{G}_N = \left\{ g_{N,n} \right\}_{n=0}^{2N}$ with

$$g_{N,n}(u) = \frac{P_{N,n}(u)}{(1+u^2)^{N+\frac{3}{2}}} \quad (22)$$

with $P_{N,n}$ given by Eqs. (18), (19), (21) is an orthonormal basis of the source space for the natural inner product.

It can be remarked that the basis functions can be expressed thanks to Gegenbauer polynomials [13, Eq. 22.3.4]

$$g_{N,n}(u) \propto \left(1+u^2\right)^{\frac{n-3}{2}-N} C_n^{(2N-n+3)} \left(\frac{u}{\sqrt{1+u^2}} \right)$$

This writing can be useful for numerical calculations, since Gegenbauer polynomials are widely implemented in many numerical software.

V. Short Study of the Basis

Let us denote by $\boldsymbol{G}_N$ the matrix whose rows are formed by the sampling of the $g_{n,N}$. The inner product between the rows, normalized by the sampling period, can be interpreted as a Riemann approximation of the continuous inner product. Therefore, there is no reason that the Gram-matrix $\boldsymbol{G}_N \boldsymbol{G}_N^t$ precisely equals the identity matrix $\boldsymbol{I}$ as expected for the easiness of the receptor implementation presented in Eq. (14).

In order to measure the orthonormality discrepancy in $\boldsymbol{E}_N = \boldsymbol{G}_N$, compared to that induced by the GS orthormalization of the initial sampled basis $\boldsymbol{F}_N$ or of $\boldsymbol{G}_N$, respectively $\boldsymbol{E}_N = \boldsymbol{F}_N^{\text{gs}}$ and $\boldsymbol{E}_N = \boldsymbol{G}_N^{\text{gs}}$, we compute the Frobenius distance $\|\boldsymbol{E}_N \boldsymbol{E}_N^t - \boldsymbol{I}\|_F$ between the Gram-matrices $\boldsymbol{E}_N \boldsymbol{E}_N^t$ and the identity $\boldsymbol{I}$. This distance is represented in logarithmic scale in Fig. 2, w.r.t. N for $u \in [-10\,,\,10]$ sampled on $K = 1000$ points.

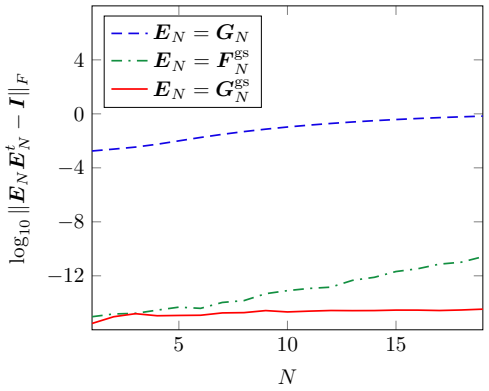

Fig. 2. Frobenius distance between Gram-matrice of $\boldsymbol{E}_N$ and identity, for $\boldsymbol{E}_N = \boldsymbol{G}_N, \boldsymbol{F}_N^{\text{gs}}$ or $\boldsymbol{G}_N^{\text{gs}}$ w.r.t. N.

Figure 2 shows that applying the GS orthonormalization to the rows of the matrix $\boldsymbol{G}_N$ leads to the more stable orthonormalization as the order increases. The reason is that from the very start of the algorithm, the rows of matrix $\boldsymbol{G}_N$ are already relatively close to orthonormality, which limits the errors of successive projections involved in GS. Moreover, even if $\boldsymbol{G}_N^{\text{gs}}$ is closer to a Stiefel matrix than $\boldsymbol{G}_N$, we note that the latter, for reasonable orders N, is fairly equivalent to a Stiefel matrix. This result is all the more interesting that $\boldsymbol{G}_N$ comes from an intrinsic orthonormalization over $\mathbb{R}$ and not just over the window $[-10\,,\,10]$. We will see in the next section that choosing $\boldsymbol{G}_N$ instead of $\boldsymbol{F}_N^{\text{gs}}$ or $\boldsymbol{G}_N^{\text{gs}}$ to perform detection has little or no impact on the detection performance.

VI. Simulation Results

We consider a multipolar signal of maximum order $N = 4$ computed with Eq. (1) and virtually measured

by a sensor moving according to the trajectory described in Fig. 1. The 24 harmonic coefficients $a_{l,m}$ and $b_{l,m}$ are randomly drawn so that the signal power is distributed equally over the $\boldsymbol{B}^{(l)}(u), l = 1, \ldots, 4$.

As a reminder, the detector performance is assessed by detection and false alarm probabilities P_{d} and P_{fa} through the receiver operating characteristic (ROC) which is a step function for a perfect detector, and identity for the worst one. The ROC for the receiver in Eq. (15) using $\boldsymbol{E}_N = \boldsymbol{F}_N^{\mathrm{gs}}$ or $\boldsymbol{G}_N$ (without numerical orthonormalization) instead of $\boldsymbol{F}_N^{\mathrm{gs}}$, applied to the noisy multipolar signal, are depicted in Fig. 3 for various signal-to-noise ratios (SNR). The latter is defined as the ratio between the signal and noise powers that is, for a signal $\boldsymbol{s}$ and a Gaussian noise whose entries are independent and of variance σ^2:

$$\mathrm{SNR\ (dB)} = 10 \log_{10} \left(\frac{\|\boldsymbol{s}\|^2}{dK\sigma^2} \right)$$

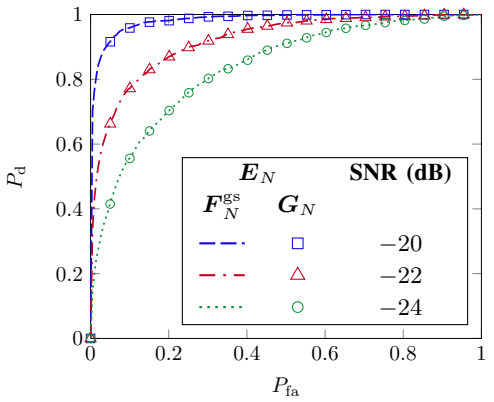

Fig. 3. ROC from Monte Carlo simulation with 2000 realizations for $\boldsymbol{E}_N = \boldsymbol{F}_N^{\mathrm{gs}}$, $\boldsymbol{G}_N$ and various SNR.

Fig. 3 shows that very close ROC are obtained for different SNR values, with the initial basis orthonormalized by GS procedure ($\boldsymbol{E}_N = \boldsymbol{F}_N^{\mathrm{gs}}$) [5] and the analytical MOBF without GS procedure ($\boldsymbol{E}_N = \boldsymbol{G}_N$). The comparison of the area under the curve (AUC) of each ROC in Fig. 3, reported in Tab. I, shows a maximal difference of 0.07% between the detectors. There is no significant impact on the detection performance to justify continuing to apply a GS orthonormalization either on the initial basis, or on the analytical MOBF, which is a very comforting result.

TABLE I
AUC (%) OF THE DETECTORS FOR DIFFERENT SNR.

	SNR (dB)					
$\boldsymbol{E}_N$	-25	. -24	-23	-22	. -21	-20
$\boldsymbol{F}_N^{\mathrm{gs}}$	78.63	83.59	87.84	92.36	96.03	98.29
$\boldsymbol{G}_N$	78.53	83.51	87.77	92.31	96.00	98.28
$\boldsymbol{G}_N^{\mathrm{gs}}$	78.63	83.59	87.84	92.36	96.03	98.29

VII. Conclusion

In this paper, the multipolar basis functions, used to describe the magnetic field produced by a fixed general source and measured on a line, have been obtained more directly than in [5] by considering the expression from [9]. In addition, we have built multipolar orthonormal basis functions based on orthogonal polynomials theory which allows to avoid orthonormalization procedures and their possible numerical instabilities. We also showed that even if the sampling process may damage the orthonormal properties of our analytical basis, they remain enough accurately satisfied even for relatively large values of the multipolar order. Finally, in terms of detection, the performances are fairly comparable to [5] and at a lower computational cost as additionnal orthonormalization procedures are not necessary.

In future work, further investigations will deal with the estimation of the CPA parameters (t_0 and D) and that of the order truncation N. In the latter case, information criteria were proposed in [5], but the theoretical impact on the performance remains to be studied.

References

[1] E. P. Loane, "Speed and depth effects in magnetic anomaly detection," *Memorandum report, ADA081329, unclassified*, 1976.

[2] R. Blanpain, "Traitement en temps feel du signal issu d'une sonde magnétométrique pour la détection d'anomalies magnétiques," PhD thesis, INP Grenoble, 1979.

[3] B. Ginzburg, L. Frumkis, and B.-Z. Kaplan, "Processing of magnetic scalar gradiometer signals using orthonormalized functions," *Sensors and Actuators A: Physical*, vol. 102, no. 1-2, pp. 67–75, 2002.

[4] A. Sheinker, L. Frumkis, B. Ginzburg, N. Salomonski, and B.-Z. Kaplan, "Magnetic anomaly detection using a three-axis magnetometer," *IEEE Transaction on Magnetics*, vol. 45, no. 1, pp. 160–167, 2009.

[5] P. Pepe, S. Zozor, L.-L. Rouve, J.-L. Coulomb, C. Serviere, and J. Muley, "Generalization of glrt-based magnetic anomaly detection," in *2015 23rd European Signal Processing Conference (EUSIPCO)*. IEEE, 2015, pp. 1930–1934.

[6] J. A. Stratton, *Electromagnetic Theory*. Hoboken, NJ, USA: Wiley-IEEE Press, 2007.

[7] G. H. Golub and C. F. V. Loan, *Matrix computations*. Baltimore: The John Hopkins University Press, 1987.

[8] S. M. Kay, *Fundamentals for Statistical Signal Processing: Detection Theory*, ser. vol. 2. Englewood Cliffs, NJ: Prentice Hall, 1998.

[9] H. González, S. Juárez, P. Kielanowski, and M. Loewe, "Multipole expansion in magnetostatics," *American Journal of Physics*, vol. 66, no. 3, pp. 228–231, 1998.

[10] M. Brazell, N. Li, C. Navasca, and C. Tamon, "Solving multilinear systems via tensor inversion," *SIAM Journal on Matrix Analysis and Applications*, vol. 34, no. 2, pp. 542–570, 2013.

[11] W. M. Lai, E. Krempl, and D. H. Rubin, *Introduction to Continuum Mechanics*. Burlington, MA, USA: Butterworth-Heinemann, 2010.

[12] J. P. Wikswo and K. R. Swinney, "A comparison of scalar multipole expansions," *Journal of Applied Physics*, vol. 56, no. 11, pp. 3039–3049, Dec. 1984.

[13] M. Abramowitz and I. A. Stegun, *Handbook of mathematical functions with formulas, graphs, and mathematical tables*. US Government printing office, 1948, vol. 55.

[14] R. P. Stanley, *Enumerative Combinatorics*. New-York, USA: Cambridge University Press, 1999, vol. 2.